11th International Symposium on Turbulence and Shear Flow Phenomena (TSFP11)
Southampton, UK, July 30 to August 2, 2019

AEROACOUSTIC NOISE GENERATION IN COMPRESSIBLE VORTEX RECONNECTION

Hamid M. M. Daryan
Mechanical and Mechatronics Engineering
University of Waterloo
200 University Ave W,Waterloo,ON N2L3G1,CA
h42moham@uwaterloo.ca

Fazle Hussain
Mechanical Engineering
Texas Tech University
2500 Broadway,Lubbock,TX 79409,USA
Fazle.Hussain@ttu.edu

Jean-Pierre Hickey
Mechanical and Mechatronics Engineering
University of Waterloo
200 University Ave W,Waterloo,ON N2L3G1,CA
jean-pierre.hickey@uwaterloo.ca

ABSTRACT

We explore the noise generation mechanisms in the compressible vortex reconnection of two anti-parallel vortices of equal strength via a high-order DNS of the fully compressible Navier-Stokes equations. Over a range of vortex Reynolds number (1500-12,000, where Re = circulation/viscosity), we show that noise generation occurs in the reconnection zone, particularly at the bridges, with a directivity in the lateral direction. A moderate correlation between the generated noise and Mach number in the vortices' advection direction is found. Finally, the simulation of $Re = 12,000$ captures at a later time a second reconnection of the small-scale thread structures reasserting vortex reconnection cascade as a realistic physical explanation of the turbulence cascade phenomenon.

INTRODUCTION

Many features of turbulent flows, like production and dissipation, fine-scale mixing, and noise generation, are rooted in the behavior of the coherent structures, their mutual interactions, and their interactions with fine-scale turbulence. In this regard, being the only known mechanism of topological change in fluid flows, reconnection of coherent structures has emerged as a central focus for many years (Hussain (1986)). Although there are still many outstanding questions about the incompressible reconnection, even less is understood about compressible reconnection–particularly about aeroacoustic noise generation.

Thus far, numerical simulations of incompressible vortex reconnection have been conducted on three canonical configurations: vortex rings (Kida *et al.* (1991)), orthogonal vortices (Boratav *et al.* (1992)), and anti-parallel vortices with a perturbation (Hussain & Duraisamy (2011); van Rees *et al.* (2012)). A noticeable aspect noted by Siggia (1985) and also others (Kida & Takaoka (1987, 1994)), is that as two vortex filaments with arbitrary orientations come close together, they twist and become locally anti-parallel. Therefore, it is reasonable to focus on this configuration as a representative canonical flow of coherent structure interaction. This simple setup allows a high-resolution simulation in order to address the fundamental features of vortical reconnection.

Melander & Hussain (1988) and Hussain & Duraisamy (2011) conducted incompressible Navier-Stokes DNS of the reconnection of two anti-parallel vortex tubes and provided some important insights. Scaling analysis clearly showed that the repulsion of the bridges is faster than the collision of the initial vortex tubes which could be justified by more intense curvature and self-induction. More interestingly, they showed that different initial conditions affect the scale factor of the vortex separation before reconnection; however, scale factor after reconnection remains the same. In other words, repulsion of the bridges is independent of the initial conditions and is dominated by the local curvature and self-induction. At higher Reynolds numbers, the curvature and the abrupt repulsion of the bridges intensify and reconnection takes place faster. It has been mentioned that such an acceleration during the repulsion phase could be considered as a source of flow-generated noise. A similar configuration was studied by van Rees *et al.* (2012) at higher Reynolds number of $Re = 10,000$. They captured the second collision of the elliptical ring which was generated as a result of the first reconnection. They demonstrated that reconnection of vortices without axial flow generates vortical structures containing axial flow. The results showed that although the general features and the main stages of the process remain unchanged, axial flow leads to an increase in the maximum circulation transfer.

Beardsell *et al.* (2016) decomposed the vorticity field into the reconnected and non-reconnected sections. In the anti-parallel configuration, they detected ring structures and associated these ring structures to the additional dipoles and instabilities at high Reynolds numbers. Newly-generated dipoles have leap-frog interactions with each other leading to off-centered viscous diffusion extrema and vortex reconnection on both sides of the symmetric plane. Beardsell *et al.* (2016) also investigated the effect of the domain size on the flow evolution of the orthogonal configuration. They found that the global physics (trend of the instantaneous

estimator of the reconnection level) remains unchanged. However, the influence of the neighboring vortices appears as slight differences in the evolution of the maximum vorticity.

Because of the additional vorticity generation mechanisms like dilatation and baroclinic terms, and the effects of the initial conditions, the compressible vortex reconnection process is more complicated. A limited number of works have considered the effects of compressibility on the dynamics of reconnection (Hussain *et al.* (1993); Virk *et al.* (1995); Shivamoggi (2006)). It has been found that shocklet formation leads to an early reconnection; however, at later times, the stretching in the bridges and the peak vorticity decrease and the circulation transfer slows down which results in a slower reconnection (Virk *et al.* (1995)). The strong dependence of compressible vortex reconnection on initial thermodynamic conditions has been examined by Virk & Hussain (1993). It has been shown that for a constant density initial condition, two dominant effects of compressibility, namely baroclinic vorticity generation and shocklet formation, cancel out during early evolution of compressible reconnection, and artificial incompressible behavior occurs. Although the initial conditions with uniform thermodynamics captures the salient features of compressible vortex reconnection, the initially unbalanced centrifugal force generates a strong acoustic wave which negatively affects the subsequent reconnection dynamics (Virk & Hussain (1993)). On the other hand, a polytropic initial condition is consistent with those observed in experiments and also minimizes the acoustic transience during compressible reconnection (Virk & Hussain (1993)).

It has been often acknowledged that mutual interaction of coherent vortical structures can play a central role in jet noise (Hussain (1983)). Laufer & Yen (1983) experimentally studied the noise radiated from a low-Mach number jet and showed that despite the moving disturbances, the acoustic sources are located at fixed positions with respect to the nozzle and are not convected. They concluded that the acoustic sources are associated with the vortex pairing locations. Although many other researchers (Crighton (1972); Williams & Kempton (1978); Kibens (1980)) had the same idea and considered vortex pairing as the main source of the jet noise, Hussain & Zaman (1981) refuted previous suggestions. They posited that the vortex pairing process is completed at distances near the exit of the jet ($x/D \approx 4$, where x is the distance from the exit of the jet and D is the diameter of the exit). However, most noise originates from farther downstream. Thus, there should be an alternative mechanism for the jet noise. They claimed that abrupt viscous reconnection with topological transformation produces most jet noise (Hussain & Zaman (1981); Hussain (1983); Hussain & Duraisamy (2011)).
It has been shown that in some particular phenomena, the primary noise sources are not necessarily dependent on the direct collision of the vortex cores. Eldredge (2007) used DNS to explore the acoustic noise generated from two-dimensional leapfrogging vortices. He showed that when the trailing vortex pair slips through the leading pair in a leapfrogging motion, an intense acoustic pulse is generated and as the vortex filaments in the outer edge of the cores are diffused, the main acoustic signal decays. Accordingly, he noted that the primary noise source in this phenomenon is related to the vortex filaments attached to the outer edge of the vortex core. He also mentioned that because of the smooth Gaussian vorticity distribution, the inner cores undergo an elastic deformation, but produce insignificant noise. It has been concluded that both initial vorticity distribution and viscous diffusion could have crucial effects on the noise generation of leapfrogging vortices (Eldredge (2007)).
Zaman (1985) conducted detailed experiments to investigate the role of the large-scale coherent structures in the noise suppression and amplification of the subsonic jet under controlled excitation. He showed that suppression takes place only for low-Reynolds number jets with initial laminar conditions. Despite Kibens (1980), who attributed noise suppression only to the localization of vortex pairing, Zaman (1985) stated that the noise suppression mechanism is also related to the initial conditions. Initial laminar coherent structures undergo more organized interactions with each other and generate higher levels of noise than the turbulent ones. Excitation of an initially laminar jet leads to an early interaction of vortices, which produces weaker coherent structures downstream. Interactions of such weaker structures generate less noise, and therefore excitation of an initially laminar jet results in noise suppression. In addition to the type of the vortex interaction, the quality and completeness of the interaction can play a central role in noise generation.
Several studies have investigated the sound generation through interactions of vortex rings. Shariff & Leonard (1992) considered two types of interaction between two vortex rings, namely passage and collision interactions. Passage interaction (in which vortex rings have the same sense of rotation and travel in the same direction) is observed in a round jet (Hussain & Zaman (1980); Zaman (1985)). Collision interaction (in which two vortex rings have opposite senses of rotation and travel toward each other) is a compact configuration of interaction of anti-parallel vortices which is believed to have an important role in the generation of jet noise (Hussain & Zaman (1981)). In this regard, many researchers studied the collision of the vortex rings experimentally (Kambe & Minota (1983); Kambe *et al.* (1993)) and numerically (Inoue *et al.* (2000); Nakashima (2008)). The role of collision and reconnection of vortex lines in the sound generation has been acknowledged in these works. More specifically, Nakashima (2008) simulated both head-on and oblique collisions of two vortex rings. He recognized that the variation of vorticity was the main source of noise and showed that for the head-on collision, a decrease in the convective velocity of the vortex ring and subsequent stretching motion generate acoustic waves. However, for the oblique collision, the second pulse is highly affected by the reconnection of the vortex lines. He found that as the collision angle becomes smaller, the reconnection of vortex lines and variation of the vorticity occur more rapidly and the second pulse is highly intensified. Note that the detailed sound generation mechanism during vortex reconnection in the three-dimensional vortical flows has not been clarified yet (Nakashima (2008)).

There is no consensus on the type of the vortex interaction that generates the most jet noise. The compressible dynamics and noise generation mechanism of the reconnection process of anti-parallel vortices remain even more unclear. Moreover, most simulations to date are limited to low Reynolds numbers and low compressibility regime. In this work, we attempt to shed some light on the dynamics of compressible reconnection and to characterize the noise generation during this process. Using DNS, we study compressible reconnection of two anti-parallel vortices over a

wide range of the Reynolds number. Locations of the noise sources, directivity of the generated noise, and any possible correlation among pressure perturbation, Mach number, and dilatation are explored. Finally, second reconnection of small-scale structures, captured for the first time with physical periodic boundary conditions, will be visualized.

NUMERICAL SETUP

Compact Gaussian vorticity distribution proposed by Virk *et al.* (1995) is used to generate the initial anti-parallel vortex tubes with a sinusoidal perturbation. This perturbation localizes the reconnection region at the middle of a $(2\pi)^3$ domain (i.e. $[-\pi,\pi]^3$) with periodic boundary conditions. The diameter of the vortex tubes equal to $d = 1.3$ and there is no gap between the vortices in the kink section. Polytropic Initial Condition (PIC) proposed by Virk & Hussain (1993) is used. Initial velocity field is computed from the vorticity distribution by using Poisson equation: $\nabla^2\vec{\mathbf{u}} = -\vec{\nabla}\times\vec{\omega}$. By assuming an incompressible and inviscid flow and substituting density by pressure based on the polytropic relation, the Poisson equation for the pressure term is obtained by taking the divergence of the momentum equation. The Poisson equation only provides the pressure difference. The pressure field is updated in a way that the pressure at the reference point (the point with the maximum velocity) becomes $p_{ref} = \frac{1}{\gamma M_{ref}^2}$, where $M_{ref} = U_{ref}/c_{ref}$ is the reference Mach number, $c_{ref} = \sqrt{\gamma p_{ref}/\rho_{ref}}$ is the reference speed of sound, and $\gamma = 1.4$. Density is determined by the polytropic relation, $p = p_{ref}\rho^{\gamma}$, which satisfies $\rho_{ref} = 1$. Reference temperature and density are thermodynamically consistent. In other words, reference pressure, density and temperature satisfy the ideal gas equation, $P_{ref} = \rho_{ref} R T_{ref}$. Reynolds number is defined as: $Re = \Gamma_{z,0}/\nu_{ref}$, where $\Gamma_{z,0}$ is the circulation of each initial vortex and ν_{ref} is the reference kinematic viscosity. In the current research, $\Gamma_{z,0}$ is constant and ν_{ref} is changed to get different Reynolds numbers. Also, the dynamic viscosity follows the power-law relation, $\mu = \mu_{ref}(T/T_{ref})^{3/4}$. Simulation time is normalized by 2π, i.e. $t = t_{sim}/2\pi$, where t_{sim} is the actual simulation time. Similar to Hussain & Duraisamy (2011), the reconnection time, t_R, is defined as the required time for the reduction of the circulation on the symmetric plane from 95% of its initial value to 50%. The time when the circulation on the symmetric plane takes 95% of its initial value is defined as the start time of the reconnection, t_S. Moreover, the time when the circulation drops to 5% of its initial value is considered as the end time of the reconnection, t_E.

Initial configuration of the problem is shown in figure 1. $z = 0$ is the symmetric plane and $y = 0$ is the collision plane. To study the directivity of the pressure perturbation, three points are considered at the middle of the three boundaries, i.e. $P1, P2, P3$ at the middle of $x = \pi, y = \pi$, and $z = \pi$, respectively. To cancel the effect of the advection of the vortices in the x direction, these points should be advected in the same direction. For this, the average of x-component of the points with the maximum vorticity on the symmetric and collision planes is set to be zero at each post-processing time step. Accordingly, the effect of the vorticities' advection at the post-processing times is cancelled and hence reconnection takes place near the middle of the domain, namely the origin of the coordinates.

We use the Hybrid code (Bermejo-Moreno *et al.* (2013)) to compute the DNS of compressible Navier-Stokes equations on our domain; the equations are closed with an ideal gas assumption; the time is explicitly advanced using a fourth-order Runge-Kutta scheme, and the spatial derivatives are evaluated using a sixth-order central finite difference scheme. In regions of high local gradients, a fifth-order WENO scheme can be used to capture the shocks. In the current study only subsonic simulations are considered; so shock-capturing scheme is not activated.

RESULTS AND DISCUSSION

Simulations are conducted for two initial Mach numbers $M_{ref} = 0.2, 0.5$, and four Reynolds numbers, $Re = 1500, 3000, 6000, 12,000$, on four grids, 384^3, 512^3, 768^3, and 1024^3, respectively. Except higher speed of sound and accordingly higher frequency of pressure perturbation, results of the lower Mach number show the same qualitative evolution as the higher Mach number. In addition, evolution of circulation, circulation change rate, and maximum vorticity on the symmetric and the collision planes essentially demonstrate the same behavior for the two considered Mach numbers. However, the amplitude of the perturbations is smaller at lower Mach number. Here, only the results of the higher Mach number, $M_{ref} = 0.5$, are discussed.

Start and reconnection time take values of $t_S = 1.32, 1.37, 1.40, 1.43$ and $t_R = 0.35, 0.24, 0.21, 0.21$ for $Re = 1500, 3000, 6000, 12,000$, respectively. Clearly, by increasing the Reynolds number, beginning of the reconnection is postponed, however, reconnection takes place more intensely such that the reconnection time decreases. The same behavior has been observed for the incompressible regime (Hussain & Duraisamy (2011)). Figure 2 shows the evolution of the pressure perturbation against time at three points, i.e. $P1, P2, P3$, for different Reynolds numbers. The general trend before reconnection is the same for all Reynolds numbers. At $P1$, in the advection direction, a jump can be seen in the amplitude of pressure perturbation near the reconnection period. At $P2$, in the lateral direction, a more intense jump is obvious at the same time. At $P3$, in the axial direction, quantities are highly affected by the motions of the vortices and a clear sudden change in the amplitude of the pressure perturbation is not captured. Therefore, generated noise directivity of the vortex reconnection is mainly oriented to the lateral direction. After reconnection, as the two new vortices (bridges) recoil from each other due to the reconnected cusp's self-induction, differences appear in the evolution of the pressure perturbations for different Reynolds numbers. Because of the periodic boundary conditions, a theoretical analysis after reconnection is not justifiable and for this purpose a larger domain should be used. However, current results clearly show the noise generation at the reconnection period for all Reynolds numbers. These results are consistent with the previous claims which consider vortex reconnection as one the most important mechanisms of jet noise generation (Hussain & Zaman (1981); Hussain & Duraisamy (2011)).

To determine the locations of the acoustic sources, based on the Powell's aeroacoustic analogy (Powell (1964)), the second time derivative of the magnitude of the Lamb vector is calculated. Iso-surface of this quantity with a minimal opacity iso-surface of enstrophy are shown in figure 3 for all Reynolds numbers at t_E. It is obvious that the approximated acoustic sources are located at the bridges, where the highly-curved reconnected vortex lines rapidly recoil by self-induction and accumulate. Such sudden re-

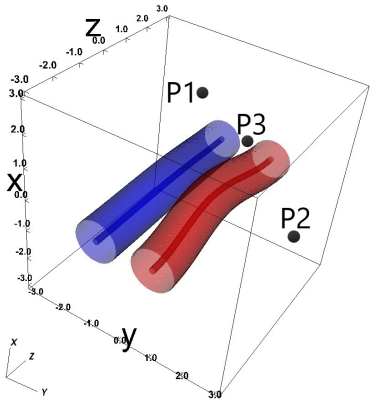

Figure 1: 3D initial axial vorticity distribution. Inner and outer surface values are 0.92 and 10^{-9} of the maximum initial axial vorticity, respectively. Rotation direction of red and blue vortices are in the positive and negative z direction, respectively. Three points, $P1, P2, P3$, are located at the middle of planes of $x = \pi, y = \pi$, and $z = \pi$, respectively.

pulsion and accordingly high level of velocity gradient introduce bridges as the moving acoustic sources during reconnection. Moreover, threads, which are small-scale vortices, survive the reconnection and experience high level of stretching; they also contribute to the acoustic noise (especially at high Reynolds numbers); see figure 3.

As it has been mentioned earlier, the amplitude of the pressure perturbations near the reconnection period is similar for all studied Reynolds numbers. To characterize the noise generation mechanism during vortex reconnection and find any scaling relation for the level of the generated noise, at the first attempt, we try to address any possible correlation between the evolution of the pressure perturbation and other variables. Considering the continuity equation for the isentropic condition, Mach number and dilatation are identified as the first candidates which may have correlations with the evolution of the pressure perturbation. After exploring the evolution of the dilatation at the considered three points, no significant correlation has been found. However, there is a correlation between the pressure perturbation and Mach number evolution. Correlation coefficients take value of $0.503, 0.144, 0.805$ at $P1, P2, P3$, respectively. In the axial direction, at $P3$, evolution of quantities is strongly affected by the vortices' motion and such strong correlation is expected. In the advection direction, at $P1$, there is a moderate correlation, which requires more analysis. In the lateral direction, at $P2$, there is not a significant correlation. Spectrum of the pressure perturbation on the center line in the advection direction is plotted in figure 4. Generation of small-scale structures at higher Reynolds number is evident.

Besides the noise generation analysis, the current study reveals the occurrence of the second reconnection between the small-scale structures for the first time. Thus far, because of the instability of the small-scale structures and generation of several dipoles, second reconnection of small-scale structures has not been captured even at high Reynolds number, $Re = 10,000$ (van Rees *et al.* (2012); Beardsell *et al.* (2016)). By imposing symmetric boundary conditions and solving a quarter of the domain, Hussain & Yao (2018) captured the second and third reconnections. In the current research, by using the physical periodic boundary conditions and continuing the simulation after the first reconnection, a second reconnection takes place for $Re = 12,000$, which is the highest studied Reynolds number for this type of the boundary condition. Figure 5 shows the evolution of the circulation change rate. Clearly, for all Reynolds numbers, there is a sudden change in the circulation change rate during the reconnection period. For $Re = 12,000$, there is a second spike at $t = 2.23$ which implies the second reconnection of small-scale structures. To visualize the reconnected small-scale structures, the simulation is continued for a longer time. Figure 6 shows the enstrophy iso-surface from different perspectives at $t = 3.18$. Separations of small ring-like structures are obvious from the right and left perspective. This phenomenon, which proves the role of the vortex reconnection in fine-scale mixing (Hussain & Duraisamy (2011)), could lead to a physical explanation of turbulence cascade through vortex reconnection scenario.

CONCLUSION

Using high-order DNS of Navier-Stokes equations, the compressible reconnection of two equal anti-parallel vortices is studied at high Reynolds numbers. Considering the evolution of the pressure perturbation in three directions, it is shown that reconnection leads to a noise generation and as it was claimed previously (Hussain & Zaman (1981); Hussain & Duraisamy (2011)), it could be considered as a dominant mechanism in jet noise. Current analysis shows that the directivity of the generated noise is mainly oriented in the lateral direction. In addition, a moderate correlation between pressure perturbation and Mach number has been found in the advection direction. It is also shown that the amplitude of the pressure perturbation spike near the reconnection period is virtually the same for all Reynolds numbers. Based on Powell's aeroacoustics analogy, approximated acoustic sources are located at the bridges, where a high level of velocity gradient is expected. Moreover, for the first time with the periodic boundary conditions, a second reconnection of the small-scale structures is captured at the highest studied Reynolds number, $Re = 12000$, which could physically explain the turbulent cascade through vortex reconnection scenario as it was claimed by Hussain & Duraisamy (2011).

Acknowledgment

This research was enabled in part by support provided by SciNet and Compute Canada.

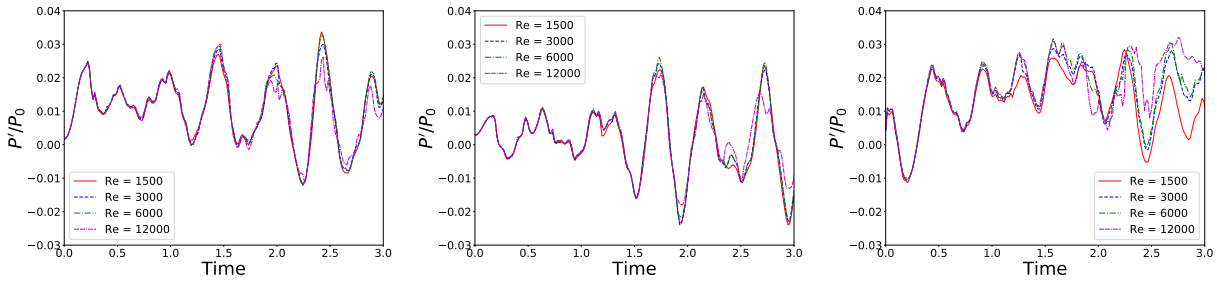

(a) Point 1 (P1) (b) Point 2 (P2) (c) Point 3 (P3)

Figure 2: Evolution of normalized pressure perturbation for different Reynolds numbers at three defined points: (a) P1, (b) P2, and (c) P3.

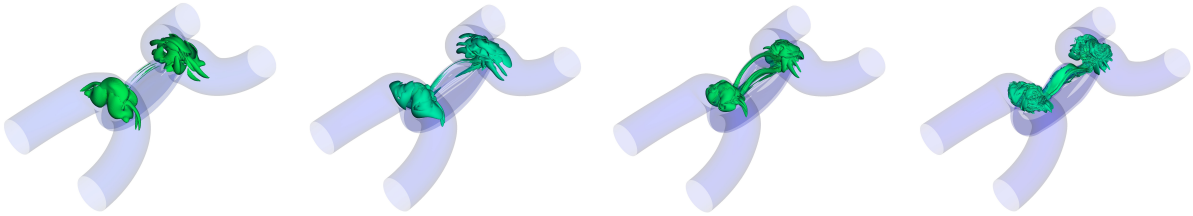

(a) $Re = 1500$ (b) $Re = 3000$ (c) $Re = 6000$ (d) $Re = 12000$

Figure 3: Locations of acoustic sources at t_E for different Reynolds numbers: (a) $Re = 1500$, (b) $Re = 3000$, (c) $Re = 6000$, and (d) $Re = 12000$. Transparent purple color is the enstrophy iso-surfec at 10% of the maximum initial axial vorticity and green color is the second time derivative of magnitude of Lamb vector at 0.3% of its maximum positive value.

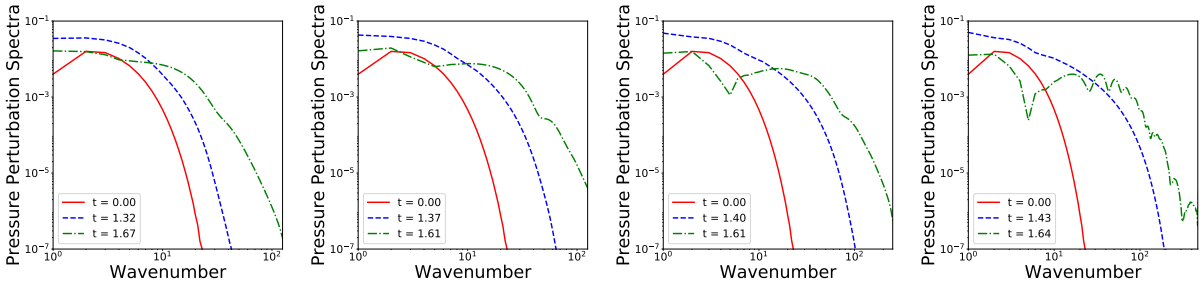

(a) $Re = 1500$ (b) $Re = 3000$ (c) $Re = 6000$ (d) $Re = 12000$

Figure 4: Spectrum of normalized pressure perturbation on the center line in the advection direction at $t = 0$ (red solid line), $t = t_S$ (blue dashed line), and $t = t_S + t_R$ (green dash-dot line) for different Reynolds numbers: (a) $Re = 1500$, (b) $Re = 3000$, (c) $Re = 6000$, and (d) $Re = 12000$.

REFERENCES

Beardsell, Guillaume, Dufresne, Louis & Dumas, Guy 2016 Investigation of the viscous reconnection phenomenon of two vortex tubes through spectral simulations. *Physics of Fluids* **28** (9), 095103.

Bermejo-Moreno, Iván, Bodart, Julien, Larsson, Johan, Barney, Blaise M, Nichols, Joseph W & Jones, Steve 2013 Solving the compressible navier-stokes equations on up to 1.97 million cores and 4.1 trillion grid points. In *Proceedings of the International Conference on High Performance Computing, Networking, Storage and Analysis*, p. 62. ACM.

Boratav, ON, Pelz, RB & Zabusky, NJ 1992 Reconnection in orthogonally interacting vortex tubes: Direct numerical simulations and quantifications. *Physics of Fluids A: Fluid Dynamics* **4** (3), 581–605.

Crighton, DG 1972 The excess noise field of subsonic jets. *Journal of Fluid Mechanics* **56** (4), 683–694.

Eldredge, Jeff D 2007 The dynamics and acoustics of viscous two-dimensional leapfrogging vortices. *Journal of sound and vibration* **301** (1-2), 74–92.

Hussain, AKMF & Zaman, KBMQ 1980 Vortex pairing in a circular jet under controlled excitation. part 2. coherent structure dynamics. *Journal of Fluid Mechanics* **101** (3), 493–544.

Hussain, AKM Fazle 1983 Coherent structuresreality and myth. *The Physics of fluids* **26** (10), 2816–2850.

Hussain, AKM Fazle 1986 Coherent structures and turbulence. *Journal of Fluid Mechanics* **173**, 303–356.

Hussain, AKM Fazle & Zaman, KBMQ 1981 The preferred modeof the axisymmetric jet. *Journal of fluid mechanics* **110**, 39–71.

Hussain, Fazle & Duraisamy, Karthik 2011 Mechanics of viscous vortex reconnection. *Physics of Fluids* **23** (2), 021701.

Hussain, Fazle, Virk, Davinder & Melander, Mogens V 1993 New studies in vortex dynamics: Incompressible and compressible vortex reconnection, core dynamics,

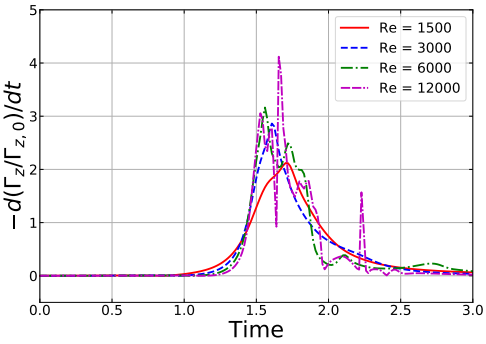

Figure 5: Evolution of normalized circulation change rate for different Reynolds numbers.

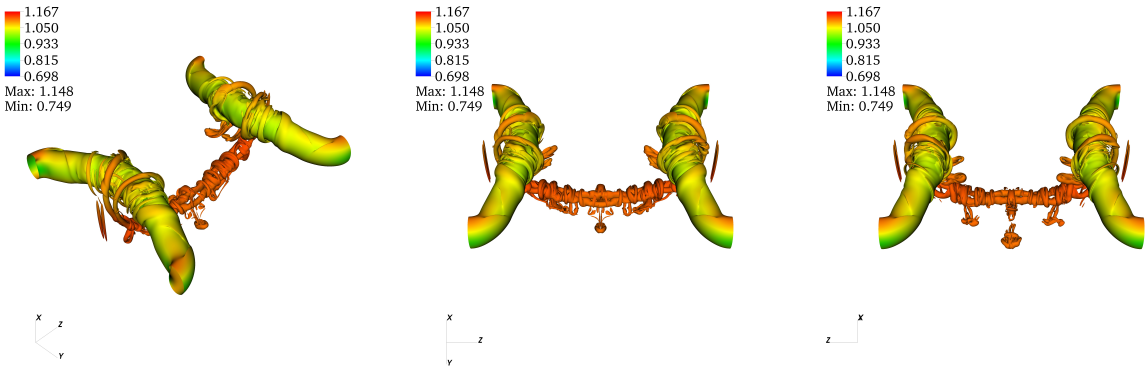

(a) Front perspective view (b) Right perspective view (c) Left perspective view

Figure 6: Enstrophy iso-surface at 15% of the maximum initial axial vorticity for $Re = 12000$ at $t = 3.18$ from different views: (a) Front perspective view, (b) Right perspective view, and (c) Left perspective view. The color represents normalized pressure, P/P_0.

and coupling between large and small scales. *Sadhana* **18** (3-4), 477–529.

Hussain, Fazle & Yao, Jie 2018 Evidence of physical turbulence cascade mechanism via reconnection cascade scenario. *Bulletin of the American Physical Society* .

Inoue, O, Hattori, Y & Sasaki, T 2000 Sound generation by coaxial collision of two vortex rings. *Journal of Fluid Mechanics* **424**, 327–365.

Kambe, T & Minota, T 1983 Acoustic wave radiated by head-on collision of two vortex rings. *Proc. R. Soc. Lond. A* **386** (1791), 277–308.

Kambe, T, Minota, T & Takaoka, M 1993 Oblique collision of two vortex rings and its acoustic emission. *Physical Review E* **48** (3), 1866.

Kibens, Valdis 1980 Discrete noise spectrum generated by acoustically excited jet. *AIAA Journal* **18** (4), 434–441.

Kida, S & Takaoka, M 1987 Bridging in vortex reconnection. *The Physics of fluids* **30** (10), 2911–2914.

Kida, Shigeo & Takaoka, M 1994 Vortex reconnection. *Annual Review of Fluid Mechanics* **26** (1), 169–177.

Kida, S, Takaoka, M & Hussain, Fazle 1991 Collision of two vortex rings. *Journal of Fluid Mechanics* **230**, 583–646.

Laufer, John & Yen, Ta-Chun 1983 Noise generation by a low-mach-number jet. *Journal of Fluid Mechanics* **134**, 1–31.

Melander, Mogens V & Hussain, Fazle 1988 Cut-and-connect of two antiparallel vortex tubes .

Nakashima, Yoshitaka 2008 Sound generation by head-on and oblique collisions of two vortex rings. *Physics of Fluids* **20** (5), 056102.

Powell, Alan 1964 Theory of vortex sound. *The journal of the acoustical society of America* **36** (1), 177–195.

van Rees, Wim M, Hussain, Fazle & Koumoutsakos, Petros 2012 Vortex tube reconnection at re= 104. *Physics of fluids* **24** (7), 075105.

Shariff, Karim & Leonard, Anthony 1992 Vortex rings. *Annual Review of Fluid Mechanics* **24** (1), 235–279.

Shivamoggi, Bhimsen K 2006 Vortex stretching and reconnection in a compressible fluid. *The European Physical Journal B-Condensed Matter and Complex Systems* **49** (4), 483.

Siggia, Eric D 1985 Collapse and amplification of a vortex filament. *The Physics of fluids* **28** (3), 794–805.

Virk, D & Hussain, Fazle 1993 Influence of initial conditions on compressible vorticity dynamics. *Theoretical and Computational Fluid Dynamics* **5** (6), 309–334.

Virk, D, Hussain, Fazle & Kerr, RM 1995 Compressible vortex reconnection. *Journal of Fluid Mechanics* **304**, 47–86.

Williams, JE Ffowcs & Kempton, AJ 1978 The noise from the large-scale structure of a jet. *Journal of Fluid Mechanics* **84** (4), 673–694.

Zaman, KBMQ 1985 Far-field noise of a subsonic jet under controlled excitation. *Journal of Fluid Mechanics* **152**, 83–111.